8-23-2019

Surface water microbial community response to the biocide 2-2-dibromo-3-nitrilopropionamide used in unconventional oil and gas extraction.

Maria Fernanda Campa
University of Tennessee, Knoxville

Stephen Techtmann
Michigan Technological University, smtechtm@mtu.edu

Mallory P Ladd
University of Tennessee, Knoxville

Jun Yan
Chinese Academy of Sciences

Megan Patterson
University of Tennessee, Knoxville

See next page for additional authors

Recommended Citation

Campa, M., Techtmann, S., Ladd, M., Yan, J., Patterson, M., Garcia de Matos Amaral, A., & et. al. (2019). Surface water microbial community response to the biocide 2-2-dibromo-3-nitrilopropionamide used in unconventional oil and gas extraction.. *Applied and environmental microbiology*. http://dx.doi.org/10.1128/AEM.01336-19

Retrieved from: https://digitalcommons.mtu.edu/michigantech-p/386

Follow this and additional works at: https://digitalcommons.mtu.edu/michigantech-p

Part of the Life Sciences Commons

Authors
Maria Fernanda Campa, Stephen Techtmann, Mallory P Ladd, Jun Yan, Megan Patterson, Amanda Garcia de Matos Amaral, and et. al.

AEM Accepted Manuscript Posted Online 23 August 2019
Appl. Environ. Microbiol. doi:10.1128/AEM.01336-19

Surface water microbial community response to the biocide 2-2-dibromo-3-nitrilopropionamide used in unconventional oil and gas extraction

Maria Fernanda Campa[1,2], Stephen M. Techtmann[3], Mallory P. Ladd[1,4], Jun Yan[5,6], Megan Patterson[6], Amanda Garcia de Matos Amaral[6], Kimberly E. Carter[7], Nikea Ulrich[8], Christopher Grant[8], Robert L. Hettich[1,4], Regina Lamendella[8], Terry Hazen[*,1,2,6,7,9,10].

[1] Bredesen Center for Interdisciplinary Research and Graduate Education, University of Tennessee, Knoxville, TN.

[2] Biosciences Division, Oak Ridge National Laboratory, Oak Ridge, TN.

[3] Department of Biological Sciences, Michigan Technological University, Houghton, MI

[4] Chemical Sciences Division, Oak Ridge National Laboratory, Oak Ridge, TN

[5] Key Laboratory of Pollution Ecology and Environmental Engineering, Institute of Applied Ecology, Chinese Academy of Sciences, Shenyang, Liaoning, P.R. China

[6] Department of Microbiology, University of Tennessee, Knoxville, TN

[7] Department of Civil and Environmental Engineering, University of Tennessee, Knoxville, TN

[8] Department of Biology, Juniata College, Huntingdon, PA

[9] Earth & Planetary Sciences, University of Tennessee, Knoxville, TN

[10] Institute for a Secure and Sustainable Environment, Knoxville, TN.

*Corresponding Author, e-mail: tchazen@utk.edu. Phone: 865-974-7709. Address: 507 SERF, University of Tennessee, Knoxville, TN 37996-1605

Abstract

Production of unconventional oil and gas continues to rise, but the effects of high-density hydraulic fracturing (HF) activity near aquatic ecosystems are not fully understood. A commonly used biocide in HF, 2,2-dibromo-3-nitrilopropionamide (DBNPA), was studied in microcosms of HF-impacted vs. HF-unimpacted surface water streams to (1) compare the microbial community response, (2) investigate DBNPA degradation products based on past HF exposure, and (3) compare the microbial community response differences and similarities between the HF biocides DBNPA and glutaraldehyde. The microbial community responded to DBNPA differently in HF-impacted vs. HF-unimpacted microcosms in terms of 16S rRNA gene copies quantified, alpha and beta diversity, and differential abundance analyses of microbial community composition through time. The difference in microbial community changes affected degradation dynamics. HF-impacted microbial communities were more sensitive to DBNPA, causing the biocide and byproducts of the degradation to persist for longer than in HF-unimpacted microcosms. Seventeen DBNPA byproducts were detected, many of them not widely known as DBNPA byproducts. Many of the believed to be uncharacterized brominated byproducts detected may pose environmental and health impacts. Similar taxa were able to tolerate glutaraldehyde and DBNPA, however DBNPA was not as effective for microbial control as indicated by a smaller overall decrease of 16S rRNA gene copies/mL after exposure to the biocide and a more diverse set of taxa was able to tolerate it. These findings suggest that past HF activity in streams can affect the microbial community response to environmental perturbation such as the biocide DBNPA.

Importance

Unconventional oil and gas activity can affect pH, total organic carbon, and microbial communities in surface water altering their ability to respond to new environmental and/or anthropogenic perturbations. These findings demonstrate that DBNPA, a common hydraulic

fracturing (HF) biocide, affects microbial communities differently as a consequence of past HF exposure, persisting longer in HF-impacted waters. These findings also demonstrate that DBNPA has low efficacy in environmental microbial communities regardless of HF impact. These findings are of interest, as understanding microbial responses is key for formulating remediation strategies in UOG impacted environments. Moreover, some of DBNPA degradation byproducts are even more toxic and recalcitrant than DBNPA itself, and this work identifies novel brominated degradation byproducts formed.

INTRODUCTION

Unconventional oil and gas (UOG) extraction has revolutionized the energy industry in the U.S. The use of hydraulic fracturing (HF) has made previously unreachable UOG reserves available for economically feasible extraction and pushed the U.S. towards energy independence (1). Multiple environmental concerns have accompanied this energy production growth. One of the most commonly added chemicals to HF fluids are biocides. Biocides are used in HF operations to control microbially-induced corrosion of casings and pipes, and gas souring caused by acid-producing and sulfate-reducing bacteria (2). However, biocides have warranted concern for several reasons. Biocides have varying degrees of reported efficacy due to potential resistance or inactivation of the biocides in HF conditions (2-5). Additionally, their toxicity and potential impact on the environment remains a contentious topic (2, 6). The fate of these biocides in the environment and their impact on microbial communities are poorly understood.

The biocide 2,2-dibromo-3-nitrilopropionamide (DBNPA) is the second most commonly used biocide in UOG after glutaraldehyde. DBNPA is a fast-acting electrophilic biocide, it is quick and effective in contact, but the protection is not long lasting (7). This biocide inhibits essential biological functions by reacting with nucleophiles (particularly sulfur-containing) inside the cell (8). DBNPA, and some of its degradation products, can also be harmful to humans and animals. These associated compounds have been demonstrated to be moderately to highly toxic by ingestion and inhalation , can be corrosive to eyes, and can cause developmental issues in terrestrial and aquatic animal studies (9, 10).

DBNPA is not toxic to all life, however, as it is biodegradable under both aerobic and anaerobic conditions, with a reported biotic half-life of fewer than 4 hours for both at neutral pH (10). However, the hydrolysis and aquatic photolysis half-life of this compound are pH-dependent, with faster degradation occurring at a more alkaline pHs. For example, the abiotic half-life of DBNPA at a pH 5, 7, and 9 is 67 days, 63 hours, and 73 minutes respectively (10). Conversely, low pH has been characteristic of HF-impacted streams (11, 12), thus providing favorable conditions for the stability of DBNPA and its degradation products.

The products of DBNPA biodegradation are the same under aerobic and anaerobic metabolism (10). Still, the relative abundance of these degradation intermediates and their reported half-lives varies depending on conditions such as pH, hydrolysis, photolysis, nucleophile presence, and aerobic or anaerobic conditions (10, 13). There are two known degradation pathways of DBNPA (Figure S1). The first pathway involves the hydrolysis of DBNPA into dibromoacetonitrile (DBAN) → dibromoacetamide (DBAM) → dibromoacetic acid. DBAN is more recalcitrant and three times more toxic than DBNPA (13). Dibromoacetic acid, a problematic disinfection-by-product (14), has a half-life of 300 days and breaks into glyoxylic acid, oxalic acid, bromide ions and carbon dioxide (15). However, a higher presence of total organic carbon (TOC) and/or nucleophilic reactions under ultraviolet light favors a second degradation pathway, where DBNPA degrades to monobromonitrilopropionamide (MBNPA), a compound two times less toxic than DBNPA (13), and then to cyanoacetamide (CAM) (13, 15). It was previously shown that HF-impacted streams have higher dissolved organic carbon than HF-unimpacted streams (16), which may impact DBNPA degradation products in impacted environments.

DBNPA can reach the environment in many ways; surface spills into the soil, surface water, and aquifers; incomplete removal after water treatment; groundwater contamination after equipment failure (leakage), and unintended fractures or abandoned wells (2). DBNPA environmental contamination could also occur in several of the steps associated with HF operations e.g., the transportation of chemicals to the site; mixing of HF fluids and chemicals on site; subsurface injection of the HF fluids; handling, collection, and storage of produce water; and disposal of the produced water (17). Understanding the impacts of surface and shallow groundwater spills, leaks, and disposal of poorly treated HF wastewater in the environment is of great concern as several studies have reported cases of the accumulation of toxic chemicals (such as hydrocarbons, benzene, toluene, ethylbenzene, and xylene, diesel, chlorinated solvents, among others) in groundwater, streams, soils, and sediments at HF operating sites (18-22). However, no study has investigated DBNPA degradation by-products and the microbial community changes over time in aerobic stream waters impacted by HF. This study aims to (1) understand the differences in local stream microbial community responses to DBNPA, (2) identification of DBNPA degradation by-products in streams impacted and unimpacted by HF operations, and (3) compare the microbial community response differences and similarities between the HF biocides DBNPA and glutaraldehyde.

RESULTS AND DISCUSSION

Quantification of bacterial 16S rRNA gene abundance over time

The 16S rRNA gene abundance was quantified at various points through the course of the experiment (Figure 1). Prior to DBNPA addition, the starting mean 16S rRNA gene concentrations were $4.03 \pm 0.60 \times 10^4$ gene copies/mL in the HF- impacted streams microcosms (HF+) and $4.38 \pm 0.50 \times 10^4$ gene copies/mL in HF-unimpacted streams microcosms (HF-). This difference was not statistically significant. Bacterial 16S rRNA gene in microcosms from two HF+ streams (Little Laurel, LL and Naval Hollow, NH) decrease immediately following addition of DBNPA and then increase, while Alex Branch (AB) displayed an increase in bacterial 16S rRNA gene concentration by day 7. In contrast 16S rRNA gene abundance in microcosms from two HF- streams (East Elk, EE and West Elk, WE) increase, while Dixon Run (DR) experienced a decrease in 16S rRNA gene concentration by day 7. Specifically, seven days after addition of DBNPA an average decrease of – 0.16 $\log_2$ fold change (FC) in 16S rRNA gene copies/mL was observed in HF+ microcosms, and a small average increase of 0.22 $\log_2$ FC was observed in HF- microcosms, indicating more sensitivity to DBNPA in HF+ microcosms. However, by day 56 the HF+ experienced a 4.9 $\log_2$ FC and HF- experienced a 3.9 $\log_2$ FC. The difference in averaged 16S rRNA gene copies/mL through time (day 7 to 56) between HF+ and HF- microcosms was statistically significant ($p < 0.05$). At day 56, the HF+ and HF- controls (no DBNPA added microcosms) were not significantly different from each other, both experienced an 8.3 $\log_2$ FC from the initial gene copies/mL at day zero. The similitude in starting microbial abundance prior to DBNPA addition indicates that the difference in microbial abundance observed after DBNPA addition was due to the initial impact of DBNPA on the microbial community, followed by its response and adaptation to the biocide, and low biocidal activity of DBNPA over time.

Quantification of the 16S rRNA gene shows that the HF- microbial communities were initially more resistant and/or tolerant to the DBNPA perturbation, as shown by the overall positive log-fold change in the gene copy number at day 7. DBNPA is a fast-kill biocide, thus resistance at the initial time point is indicative of inefficacy of microbial control in HF- microcosms. Through time, both HF- and HF+ showed strong resilience and adaptation to decreasing concentration of DBNPA, however by day 56 HF+ had an overall greater gene copies/mL (Figure 1) and the log-fold change than HF-.

There is no indication that the HF+ streams had any prior exposure to DBNPA prior to this experiment. UOG operators in the area have disclosed the use of other biocides, such as glutaraldehyde (reported in self-disclosing website fracfocus.org). Thus, prior exposure to HF activity, not containing DBNPA, did not appear to provide ‘priming’ or a competitive advantage to DBNPA exposure based on 16S rRNA gene copies/mL alone, but it provided favorable conditions for quicker resilience (23). Furthermore, quantification of the 16S rRNA gene copy number shows that there is overall environmental tolerance to high concentration of DBNPA, indicating DBNPA is not as effective in controlling complex and dynamic microbial communities as compared to environmental isolates or engineered systems (9, 24).

Microbial Community Structural Changes

Microorganisms in headwater ecosystems are environmental regulators of natural geochemical cycles and organic matter cycling (25, 26). Microorganisms are very sensitive to perturbation making them good sensors of environmental change and effective for tracking contaminants (27). Before DBNPA addition HF- microcosms had an overall higher evenness and richness than HF+. After addition of DBNPA, evenness and richness were affected through time in both HF+ and HF- microcosms. Shannon diversity, which account for the abundance and evenness of species present, showed that HF+ microcosms experienced a smaller decrease in evenness and richness—even though HF- had an overall higher diversity (Figure 2a) ($P < 0.01$). Meanwhile, while not statistically significant, Simpson diversity (Figure 2d) which also accounts for the abundance of species present, indicated minimal changes in diversity over time except for HF- at day 21. Still, diversity increased by day 35. In contrast, Chao1 ($P < 0.05$) and Observed ($P < 0.05$) measurements (Figure 2b and 2c), which include unique and rare operational taxonomic units (OTUs) in their calculations, experienced a more prominent decrease in diversity, as fewer OTUs dominated over time. In contrast, when comparing day zero with day 56 control to test bottle effect, the changes detected by day were not significant, and HF- maintained higher diversity than HF+.

Analysis of weighted UniFrac distances between samples revealed that there was a difference in phylogenetic composition response between HF+ and HF- microbial populations. The weighted UniFrac distances were plotted on a directional Principal Coordinate Analysis (PCoA), PC 1, explained 27.90 % of the sample variance, while PC2, explained 17.99% of the sample variance (Figure 3). At day zero, prior to DBNPA addition HF+ and HF- already clustered separately along the PC1 axis, but after DBNPA addition HF+ and HF- visibly separated more over time, showing that the HF+ and HF- got more dissimilar over time after addition of DBNPA.

Meanwhile the HF+ and HF- no-DBNPA added controls cluster together at day 56. Permutational multivariate analysis of variance (PERMANOVA) indicated that there were statistically significant differences between HF+ and HF- microbial community through time (Table 1). This difference indicates that DBNPA selected for different sets of taxa based on HF exposure.

Differentially Enriched Taxa Over Time and Between HF+ and HF- Microcosms

The initial bacterial population (before DBNPA amendment) in all microcosms, regardless of HF history, was predominantly *Proteobacteria*, which comprised more than 75.5% ± 4.8% of 16S rRNA gene reads in HF+ and more than 64.4% ± 3.2% in the HF- group. *Proteobacteria* were expected to dominate, as previous studies on these Pennsylvania streams reported this phylum as the principal population (11, 12, 16). However, initial proportions of *Beta*, *Alpha*, and *Gammaproteobacteria,* in that order of abundance differed between the HF+ and HF- groups. Taxa plots illustrate the difference in microbial community structure over time (Figure S2a and S2b). *Gammaproteobacteria* were the first responders in both HF and HF- after 7 days of DBNPA addition with *Pseudoalteromonadaceae* as the most dominant family at this time, 12.3% ± 4.0% of HF+ microcosms and 19.4% ± 2.2% of HF- microcosms. A strong correlation between *Gammaproteobacteria* and HF+ streams has been shown before (11, 12). By day 35, *Alphaproteobacteria,* specifically, the genus *Methylobacterium* was the most dominant taxa (15.6% ± 7.7% in HF+ and 30.5% ± 6.2% in HF-). However, by day 56 a more diverse microbial composition was observed, with few overall dominant taxa. In HF+ the most dominant taxa were Unclassified bacteria (10% ± 5.1%) , *Comamonadaceae* (9.5% ± 2.7%), *Alcanivoracaceae* (8.9% ± 7.8%), and *Sphingomonadaceae* (7.9% ± 2.4%), and in HF- the most dominant taxa were *Comamonadaceae* (6.3% ± 0.8%), auto67_4w from the order *Pedosphaerales* (5.7% ± 1.3%), and *Methylobacteriaceae* (6.3% ± 2.7%) (Figure 4).

There were important changes to the microbial community structure in both HF+ and HF- following amendment with DBNPA. Seven days after DBNPA amendment, the relative abundance of 29 taxa were significantly different (DESeq2, Wald Test P=> 0.01) in both HF+

and HF- compared to day zero; 24 of which increased in relative abundance, and five decreased (Table S1). The two taxa with the highest increase were identified as the family AEGEAN 185 (7.43 log_2FC) from the SAR404 phylum, and family SAR 324 (7.26 log_2FC) a member of the class *Deltaproteobacteria*. Both of these taxa were reported in a similar experiment using the biocide glutaraldehyde (28). AEGEAN 185 matches to sequences of a clone library from the North Aegean Sea, but its metabolic profile is unknown (29). Sequenced members of SAR 324 are known to possess genes for methane monooxygenase and dehalogenases that, if expressed, can co-metabolize halogenated compounds such as DBNPA (30-32). The only enriched genus with a relative abundance greater than 2% at all time points in the experiment was *Alcanivorax* (3.27 log_2FC). *Alcanivorax* is a known oil degrader (33) and was also enriched in glutaraldehyde microcosms, showing a wide range of xenobiotic compounds it is capable of tolerating, and even possibly degrading (28). In addition to the three previously mentioned taxa, 9 more were enriched with both glutaraldehyde and DBNPA: *Achromobacter, Synechococcus,* SarSea-WGS and Artic95A-2 from the SAR 406 clade, *Acidimicrobiales, Nitrospina, Sphingopyxis* and *Euryarchaeota* Marine group II and III. Of the five suppressed OTUs, three were from the order *Burkholderiales.* Differential abundance analysis between HF+ and HF- at day 7 showed 51 taxa were significantly different; 30 were enriched in HF+, and 21 were enriched in HF- (Table S2). The most substantial log FC was *Micrococcus* (6.14 log_2FC), and the taxa that were enriched and comprised more than 2% relative abundance in HF+ were *Verrucomicrobiaceae, Caulobacteraceae, Janthinobacterium, Novosphingobium, Oxalobacteraceae,* and *Limnohabitans.*

The microbial communities at days 21, 35, 49, and 56 (Tables S3, S4, S5, and S6, respectively) followed a similar trend, with approximately 100 differentially enriched taxa in both HF+ and HF- microcosms compared to day zero. Through time, many OTUs related to marine environments such as *Idiomarina,* SAR 324, Aegean-185, *Alteromondaceae,* ZD017, *Halomonas,* and *Alcanivorax* were enriched. Enrichment of marine taxa is notable as osmotic regulation and efflux pumps, which are important attributes of marine microbes, have been linked to biocide tolerance (34-37) but mechanistic details about microbial tolerance to DBNPA have not been previously reported. Marine organisms are found in low abundance in freshwater streams, and they can bloom when conditions are favorable (38), which indicates a potential competitive advantage of halotolerant bacteria to DBNPA. For example, a halotolerant *Halomonadaceae* was shown to be enriched in HF exposed anaerobic sediments treated with DBNPA (39). Other halotolerant bacteria have also emerged as bacterial biomarkers of UOG impacts in freshwater streams (40). HF fluids contain high abundance of halophilic and halotolerant bacteria (41), which can be displaced to streams in the event of an HF fluid spill.

Other differently enriched organisms between days 21, 35, 49, and 56 (Tables S3, S4, S5, and S6, respectively) included *Dietzia, Bacillus, Methylobacterium, Verrucomicrobiaceae, Novosphingobium, Caulobacteracea,* among others. *Dietzia* was previously shown to resist antimicrobials in freshwater and wastewater ecosystems (42). *Bacillus* has been reported to possess intrinsic resistance to antimicrobial as they can form spores when antimicrobial pressure is encounter (43, 44). Bacterial spores are the least susceptible to biocidal action (43). *Methylobacterium* is a common environmental microbe that was previously shown to be enriched and dominant after freshwater consortium was exposed to glutaraldehyde (28), and species in this genus have been shown to be resistant to other antimicrobials (45). Another microcosms study using sediment and water anaerobic mixture showed that DBNPA exposure decreased *Methylobacteriaceae* abundance (39), indicating that oxygen availability is needed for *Methylobacterium* resistance and enrichment in the presence of DBNPA. *Novosphingobium* are commonly found in environments impacted by anthropogenic activity (46). They are known to be effective biodegraders of toxic and recalcitrant compounds (46). However, the family *Sphingomonadaceae*, which *Novosphingobium* is a member of, also was shown to decrease after exposure to DBNPA in a previous anaerobic sediment and water microcosms (39), indicating again that oxygen or sediment presence affect tolerance and resistance of this taxa. Taxa enriched in HF+ but not HF- included *Verrumicrobiaceae* and *Caulobacteraceae* which were shown by another study to be susceptible to a low dosage of DBNPA in sediments that were not exposed to HF (39). The enrichment of these taxa only in HF+ microcosms may indicate that prior exposure to HF fluids can build tolerance to DBNPA in *Verrimicrobiaceae* and *Caulobacteraceae* regardless if HF fluids contained DBNPA. Furthermore, *Caulobacteraceae* has been previously identified as a microbial biomarker of UOG activity in streams in PA (40).

At day 56, the negative control had 209 differentially enriched taxa compared to day zero, which can be attributed to bottle effect (Table S11). Meanwhile, at day 56 the experimental and negative control microcosms (no DBNPA added) had 181 differentially enriched taxa. Of those, 111 were enriched in the experimental microcosms (Table S12), which, when summarized at genus level, reveals that *Bacillus, Idiomarina, Glaciecola, Alcanivorax, Acinetobacter, Vibrio, Dietzia, Methylobacterium, Pseudoalteromonas, Marinobacter, Novosphingobium, Stenotrophomonas, Burkholderia, and Oxalobacteraceae (unclassified genus)* show tolerance and adaptation to DBNPA.

Another study used .0025% v/v DBNPA with and without the addition of FeOOH in anaerobic microcosms constructed with sediment inoculum from up- and downstream from a UOG wastewater treatment facility to understand how UOG wastewater processing affects downstream microbial communities and how those changes affect anaerobic microbial responses to HF fluid additives (39).That study found three enriched families in the UOG-downstream microcosms amended with only DBNPA and two of those, *Halomonadaceae* and *Staphylococcaceae,* were also found in this study. Conversely, the same UOG downstream samples were amended with FeOOH and DBNPA, and six families were enriched, two of which were also detected in this study: *Rhodospirillaceae* (enriched over time in HF+ as compared to HF-, Tables S2, S7 to S10), and *Ignavibacteriaceae* (enriched at days 21and 35, Table S3 and S4). However, the study by Mumford et al. (2018) only sample at day 42 after incubation, and the low DBNPA concentration, sediment, and anaerobic conditions used are expected to result in wide differences between that study and the one described here.

Microbial community responses to DBNPA vs. Glutaraldehyde

We recently conducted a similar study using 100 mg/L of the biocide glutaraldehyde (28). The changes in microbial abundance observed after treatment with DBNPA contrast with the results of the glutaraldehyde experiment. In the glutaraldehyde study, all of the six stream microcosms experienced an initial decrease in microbial abundance. On average HF+ communities were initially more resistant to the biocide, as observed by a smaller log-fold change of 16S rRNA gene/mL by day 7. By day 56, HF- showed stronger resilience by having a bigger positive log-fold change. These results show that the microbial abundance adaptation response in these microbial communities is biocide specific.

Methylobacterium, Idiomarina, Bacillus, and Alcanivorax, among others, were enriched in the presence of both DBNPA and glutaraldehyde (28). The enrichments indicate that these taxa have a competitive advantage when exposed to these two electrophilic biocides. Previous studies have shown that glutaraldehyde resistance may be caused by the expression of efflux pumps (36, 47). However, the mechanisms for DBNPA resistance is not known, and functional genomics and transcriptomics analyses are needed to better understand this mechanism.

Furthermore, Weighted UniFrac beta diversity (Figure 3) showed a distinct phylogenetic response between HF+ and HF- microcosms. This was similar to what was observed in previous work (28), yet glutaraldehyde showed more significant phylogenetic distances on a PCoA plot. The primary axis explained 65.4 % of the variation and the second axis explained 10%, while for DBNPA PC1 and PC2 explained 27.90% and 17.99% respectively, showing that the response and phylogenetic changes due to DBNPA addition were not as pronounced as for glutaraldehyde. Even though both are electrophilic biocides, DBNPA is a fast kill biocide while glutaraldehyde biocidal properties are longer lasting (2). Glutaraldehyde is also more persistent over time (28), with a biotic half-life of 33.8 d in HF- and a biotic half-life of 51.9 in HF+, potentially explaining the more pronounced differences in the phylogenetic distribution of glutaraldehyde-treated microcosms over time. Furthermore, the alpha diversity changes and the differentially enriched taxa suggested that the microcosms contain a higher quantity of OTUs that are able to tolerate and adapt to DBNPA as compared to having just a few OTUs becoming enriched as it the case of glutaraldehyde (28). For example, *Methylobacterium* was the most dominant taxa by day 35 in the microcosms exposed to DBNPA (15.6% in HF+ and 30.5% in HF-) , but by day 56 there is not clear dominating taxa. In contrast, when exposed to glutaraldehyde *Methylobacterium* dominated the community from day 21 throughout day 56. At this final time point *Methylobacterium* represented 70.6% of the observed microbial community HF+ and 84.2% in HF- (28). Based on this comparison, combined with the significant increase in 16S rRNA gene copies, it seems that DBNPA tolerance is more ubiquitous. There are multiple possible explanations for this result: (1) changes in the microbial community structure and/or adaptation of individual community members improves resilience of the community as a whole, and (2) DBNPA is degraded either biotically or abiotically more rapidly than glutaraldehyde (28, 48, 49).

Abiotic and Biotic Transformation of DBNPA

We evaluated the degradation of DBNPA over 56 days (d) using both biotic and abiotic microcosms constructed from HF+ and HF- streams (Figure S3 and Figure S4). However, the degradation rate of DBNPA could not be calculated as quantification by HPLC-DAD revealed a sharp increase in DBNPA signal at day 14 at two of the HF+ sites with documented spills (AB and LL, both biotic and abiotic samples). The sharp increase in DBNPA signal could not be attributed to human error, or equipment malfunction (Figure S3 and Figure S4). It is possible that a coeluting compound was absorbed in the same region or interfered with the HPLC-DAD measurement, which could explain the spike at day 14 (Figure S4), due to chromophores and/or similar degradation products that may not be distinguishable with this method (50) . However, DBNPA non-detection was achieved by all HF- biotic microcosms sets (28 d for EE, 49 d for WE, and 56 d for DR), while only one HF+ biotic microcosm set reached non-detection (56 d for

NH). Conversely, only one HF- abiotic microcosms set reached DBNPA non-detection (49 d for EE) and only one HF+ abiotic microcosm set (56 d for NH). These observations indicate HF- microbial communities were better at tolerating and degrading DBNPA.

DBNPA degradation has been documented previously (10, 13, 15). It was shown by others that degradation rate of this biocide in pH dependent with degradation rates inversely proportional to pH (10, 15). In this study, HF+ streams had an average pH of 4.9 ± 0.13 and HF- streams had a pH of 6.5 ± 0.46 (Table S15), and HF- microcosms depleted DBNPA faster than HF+ which agrees with the pH dependent degradation trends previously reported(10, 15). The only biotic HF+ microcosm set to reach non-detect was NH which had the least acidic pH of the set (Table S15). However pH based hydrolysis was not the only factor contributing to degradation as abiotic microcosms were not able to reach non-detect at the same speed, indicating microbial biodegradation also played a role.

To evaluate whether a contaminant or degradation product with similar absorbance and retention time as DBNPA may be contributing to the DBNPA signal, the biotic and abiotic samples from days 0, 7, 14, 21, and 28 from the HF+ sites (AB and LL) and also two HF- sites for comparison (WE and EE) were analyzed using nano-HPLC-HRMS. High mass accuracy measurements (+/- 5 ppm) and fragmentation data from the LC-MS were used to qualitatively evaluate the results, first by searching for DBNPA and known degradation products, and then by comparing the number of brominated compounds detected. Then, relative abundance values and integrated peak area were used to evaluate the trends of these compounds across the five time points within each sample set. The DBNPA molecular ion ($[M+H]^+$ = 240.8606 *m/z*) was not detected in most of the samples analyzed, which may be due to prolonged storage or multiple freeze-thaw cycles (each sample experienced 2 freeze-thaw cycles). However, because bromine (Br) has a unique isotopic signature (Figure S5), multiple other brominated species were observed; some of which were known DBNPA degradation products, but many were previously-unreported species and potentially novel brominated degradation products (Table S13). Across the four sites (WE, EE, AB, LL), five time points (day zero to 28), and two microcosm conditions (biotic or abiotic) analyzed (n = 40), 18 brominated species were observed, including DBNPA and four known degradation products: CAM, MBNPA, DBAN, and DBAM (Figure S1, Table S13). The detected mass to charge ratio, predicted elemental formula, and putative structure of some of these brominated products are described in Table S13. More brominated species were detected in the abiotic samples (an average of 14.1 ± 2.8) compared to the biotic samples (11.7 ± 4.4) (Figure S6). There were also more brominated species in the biotic HF- samples (13 ± 5.6) than the biotic HF+ samples (10.4 ± 3.3) and in abiotic HF- samples (15.2 ± 3.5) than the abiotic HF+ samples (13 ± 1.7) (Figure S6). Number of brominated compounds increased through time in all samples (Figure 4), indicating the formation of byproducts of degradation or reaction of bromide with available organics in the water. Similar to the trend observed by HPLC-DAD, the number of brominated species detected by LC-MS in the HF+ abiotic samples (AB and LL) increased sharply from day zero to day 14 (Figure S6). The total “brominated signal” (summed, integrated peak areas at each time point) also increased sharply at day 14 in the abiotic HF+ samples (Figure S7). While not as strong, the brominated signal also increased at day 14 in the two abiotic HF- samples. For the biotic samples, a steady increase in brominated signal over time was observed regardless of the microcosm, with the highest signal occurring at day 21. The qualitative trends are consistent with the initial HPLC-DAD measurement, which suggests that these brominated degradation products may indeed have impacted the signal response in the initial measurement.

MBNPA and CAM, two known degradation products of the less toxic degradation pathway (Figure S1), were detected in abiotic and biotic in both HF+ microcosms (AB and LL) and one HF- (EE). DBAN, toxic pathway degradation product (Figure S1) was detected in the biotic LL microcosms (HF+) and abiotic and biotic EE microcosms (HF-), while DBAM, another toxic degradation pathway product, was detected in both biotic AB and LL (HF+) and only abiotic LL, while both abiotic and biotic WE and EE (HF-). Others have shown that the preference for one degradation pathway is dependent on total organic carbon (TOC) content, and that higher TOC selects for the less toxic pathway, with MBNPA as an intermediate (13). It is documented that HF+ streams in PA, including AB and LL, have higher dissolved organic carbon than HF- due to land clearing practices from well-pad development (16). Here, mean TOC (Table S14) at day zero was significantly higher in HF+ samples (7.81 ± 1.11 mg/L) than in HF- samples (4.09 ± 0.95 mg/L; *t*-test, P = 0.02), which could explain the presence of the nontoxic pathway intermediates at the HF+ microcosms, TOC could also be reacting with bromine left after complete DBNPA degradation. Other factors to consider include different enzymatic capabilities of the microbial communities present within the samples or different water chemistries favoring one pathway over another. The water chemistry measured *in situ* (Table S15) was reported previously: temperature (HF+: 16.8°C ± 1.96, HF-: 12.8°C ± 0.58), pH (HF+: 4.9 ± 0.13, HF-: 6.5 ± 0.46), conductivity (HF+: 29.2 ± 3.67μS/cm, HF-: 33.7 ± 5.66 μS/cm), and total dissolved solids (HF+: 20.8 ± 2.80 mg/L, HF-: 23.9 ± 4.01 mg/L) (28). Even though the differences in these parameters were not significantly different between HF+ and HF-, the differences in pH may affect the stability of DBNPA as discussed previously. This observation is also supported by cluster analysis as the detected brominated species clustered by HF impact history (Figure 5a). Samples also clustered by biotic and abiotic conditions per stream, indicating that microbial presence affected the degradation byproducts (Figure 5b). Overall, these results suggest that DBAM and other brominated species may be persistent degradation products of DBNPA that, depending on the history of the watershed, may be preferentially selected over the desired less toxic pathway with MBAN and CAM as intermediates. More DBNPA degradation kinetic experiments are needed to better understand the conditions dictating intermediate formation.

Environmental Implications

Our findings demonstrate that previous HF exposure causes surface water microbial communities to respond differently to the biocide DBNPA as compared to HF-unimpacted communities. HF exposure history, and its effect in water chemistry and microbial interactions, may also affect the formation of DBNPA brominated degradation products. In a similar experiment using glutaraldehyde, a distinct microbial community was enriched between HF+ and HF- after glutaraldehyde perturbation. In the glutaraldehyde experiment the HF+ microbial community showed higher tolerance to glutaraldehyde based on higher diversity and a smaller log fold decrease of the 16S rRNA gene concentration, but HF- microbial community was able to degrade glutaraldehyde faster. The faster glutaraldehyde biodegradation in HF- was attributed to biotic-abiotic interactions as HF+ had acidic pH compared to HF- (28), as glutaraldehyde activity is enhanced at alkaline pH (51). Alkaline pH forms more reactive sites in the cell wall, this effect allows more bacteria to be susceptible to glutaraldehyde while depleting the glutaraldehyde in solution as it cross-links with the bacterial wall (51).

DBNPA caused a different microbial response than the biocide glutaraldehyde. First, HF- microcosms were better at tolerating DBNPA based on initial 16S rRNA log fold change, which is opposite to what was observed with glutaraldehyde. This could be in part due to DBNPA faster hydrolysis at increasing pH, causing HF- microcosms to deplete DBNPA faster as compare to the more acidic HF+ microcosms. Second, even though similar microbial groups were enriched, a more diverse microbial population was able to resist DBNPA as compared to glutaraldehyde, as *Methylobacterium* enrichment represented up to 92% of glutaraldehyde microcosms (28). The difference in microbial response may be caused by the DBNPA fast-kill approach, where its biocidal activity is more potent at the moment of initial contact, while glutaraldehyde works over a period of days to weeks. However, both DBNPA and glutaraldehyde depletion was faster in HF- microcosms.

This study revealed that DBNPA and associated degradation products can be persistent in stream water. TOC could have a role in the formation of degradation products. These findings are of importance, as environmental persistence may further hinder the return of the microbial communities to pre-impacted states affecting nutrient cycle, and further retard microbial natural biodegradation capabilities (i.e. microbial attenuation) in the environment, potentially requiring intervention to stimulate the affected area to enhance the preference for DBNPA non-toxic degradation pathways. Environmental persistence of the brominated disinfectant by-products can cause harm to the public and environmental health. For example, the persistence of these disinfectant by-products may affect ecosystem function, e.g. microbial primary production and natural attenuation which could have unknown cascading effects to higher trophic levels (10, 52-55). Broad HF impacts have already been shown to affect micro and macroinvertebrates, fish and other aquatic organisms in the streams used as source water for the microcosms (16, 56).

Many of the taxa enriched in this study have been previously reported as being capable of degrading or co-metabolizing xenobiotic compounds. Although a genetic pathways for microbial biodegradation of DBNPA has not been determined, as a halogenated compound, it is likely that the aerobic degradation pathways would involve cometabolism, aerobic assimilation, or dehalogenation (57, 58). In the non-toxic degradation pathway of DBNPA (Figure S1), the bromines are substituted by hydrogen, which could be achieved by microbial reductive dehalogenation (59), and by abiotic mechanisms. For example, AB and LL (HF+ streams) derived microcosms showed intermediates of the less toxic degradation pathway, in both biotic and abiotic conditions, but MBNPA was an order of magnitude higher in biotic conditions (Figure 5b), leading to the conclusion that microbial biodegradation is active and rapid compared to abiotic degradation alone. Further research is needed to understand which microbes can use DBNPA as a carbon source, electron donor, or electron acceptor in metabolism.

Additional research is needed to determine a complete degradation pathway, including quantification of all brominated intermediates, and to better understand when one DBNPA degradation pathway is preferred over the other to adequately handle a HF chemical spill containing DBNPA. Furthermore, differences in degradation kinetics of DBNPA and associate degradation products between HF+ watersheds and pristine should be determined to quantify and determine under what conditions HF+ microbial communities are more efficient at debrominating

DBNPA and its degradation byproducts. DBNPA may not persist in the environment, but its brominated degradation products, such as DBAN, have a longer half-life and could be more harmful to the public and environmental health.

MATERIALS AND METHODS

Stream Selection and Sample Collection

For comparison purposes, sample collection was identical and done at the same time as Campa et al., 2018 . Briefly, sample selection employed GIS surveys, and the Pennsylvania Department of Environmental Protection (PADEP) records to minimize watershed variation caused by industrial activities other than UOG extraction. Streams selected were in forested areas, with no indication of past mining activity or other anthropogenic impacts in the PADEP records. HF-impacted (HF+) streams had active UOG wells within the watershed. These streams were Alex Branch (AB), Little Laurel (LL), and an unnamed tributary to Naval Hollow (NH). AB and LL had reported surface spills (60-62). The spills occurred in 2009 when a pipe carrying flowback water burst, leaking into LL, and to a lesser extent to AB. In the same year, HF chemicals were accidentally spilled into AB. The three HF un-impacted (HF-) streams had construction development involving well pads, but no HF activity had started. These streams were UNT East Elk (EE), unnamed tributary to West Elk (WE), and Dixon Run (DR). Refer to Table S15 for geological coordinates of the watersheds. A detailed description of the sites, screening process and selection has been described previously (11-13, 56, 63).

Collection of stream water from three HF+ and three HF- streams in northwestern Pennsylvania occurred in June 2015 under low flow conditions. Samples were collected in sterile Nalgene bottles and stored at 4°C until use. Conductivity, pH, temperature, and total dissolved solids were measured at collection time using a weekly calibrated Eutech PCSTestr 35 Multi-parameter test probe.

Microcosm Setup

Dow Chemicals' literature showed effective kill (> 6 log reduction) of acid producing bacteria (APB) and sulfate-reducing bacteria (SRB) using 25 mg/L of DBNPA (24); nevertheless, biocide usage in HF is highly variable with reports between 10 to 800 mg/L (6). Thus, microcosms were constructed using 125 mg/L DBNPA in 235 mL of stream water. DBNPA was purchased from Sigma-Aldrich (CAS 10222-01-2). Abiotic controls were autoclaved to kill all microbes present and were used to measure abiotic degradation of DBNPA. Negative biological controls (No-DBNPA added) were used to examine the bottle effect in microbial communities with no biocide added. Abiotic and biological controls were set at a volume of 20 mL. All microcosms were set in triplicates at ambient temperature (~21°C) under aerobic conditions and minimal light exposure for 56 days. Microcosms were uncovered only for sampling events and were shaken before sampling. Samples were collected every seven days for chemical analysis and day zero, 7, 21, 35, 49, and 56 for microbial analyses. TOC was measured before the beginning of the experiment using a Shimadzu TOC-L Series analyzer with ASI-L autosampler (Shimadzu, Kyoto, Japan) following the protocol described in Campa et al., 2018.

Quantification of Bacterial 16S rRNA Gene

DNA was collected by filtering 25 mL of microcosm water through a 0.2 µm nylon filter (Sterivex), and frozen at -20°C until use. The frozen filter was cut with sterile pliers. The filter membrane was cut with a sterile razor and DNA was extracted from the membrane using Mo Bio PowerSoil DNA isolation kit following manufacturers specifications. Bacterial primers Bac1055YF and Bac1392R were used to quantify the 16S rRNA gene in a QuantStudio 12K Flex Real-Time PCR system (ThermoFisher Scientific). For reaction mixture, and qPCR parameters refer to Campa et al. (2018).

16S rRNA Gene Amplicon Library Preparation, Sequencing, and Data Analyses

After DNA extraction, the v4 region of the 16S rRNA gene was amplified using the primers and protocol described previously (64). Refer to Campa et al. (2018), for the description of library preparation. The final libraries were run in the Illumina MiSeq (San Diego, CA, USA) using a v2 (2 x 150 reads) kit following manufacturer's specifications.

Data analyses were done in QIIME (version 1.9.1) following the protocol described in Campa et al. (2018). Briefly, after joining forward and reverse reads and demultiplexing, quality filtration was set to an average Q-score of more than 19. De novo and reference-based chimera detection was done using UCHIME in the USEARCH package (65, 66). OTU picking was done using the Greengenes database (version May 2013)(67) applying a 97% sequence identity cut-off using UCLUST(65). Representative sequences for each OTU were aligned using the PyNAST method (68) and taxonomy was assigned using the RDP classifier (69). The OTU table was filtered further to remove sequences with counts below 0.005% and any samples with less than 1000 sequences were discarded and the OTU table was cumulative-sum scaling (CSS) normalized (70) for beta diversity, weighted UniFrac distance matrix calculation (71). Weighted Unifrac distance matrix was visualized using a directional Principal Coordinate Analysis (PCoA) in EMPeror (72) forcing the x-axis by days. The OTU table and weighted Unifrac was then imported into R and the packages Phyloseq (73) and Vegan (74) were used for statistical analyses as described below. An unnormalized OTU table was also exported into R for alpha diversity and DESeq2 analyses (75, 76). Difference in alpha diversity metrices, Chao 1, Simpson, Shannon, and Observed species, were computed using the package Phyloseq (73) to understand the difference in evenness and richness between HF-impacted and HF-unimpacted microcosms before and after DBNPA addition. Statistical analyses were performed as described in the next section.

DESeq2 (76) R package was used to identify differentially enriched taxa through time and between HF+ and HF- microcosms at each time point (day 7, 21, 35, 29, and 56) to day zero no-DBNPA added controls. Day 56 DBNPA added microcosms and day 56 no-DBNPA added controls were compared as well. Per time point, comparisons between HF impact status were also made. For each comparison a Wald test was performed using the parametric fit-type and the P-value was adjusted using Benjamini & Hochberg method. Reported OTUs had an alpha < 0.01 and a reported 2 log_2 fold change or higher. following the protocol in Campa et al (2018). using a cutoff of 2 log_2 fold change or higher, and a Bonferroni adjusted p-value of 0.01.

Statistics

For comparison purposes, statistical analysis was similar to that in Campa et al. (2018). To understand the effect of DBNPA on microbial community, 16S rRNA gene abundance was compared using a complete randomized design (CRD) with split plot using impact status (HF+ vs. HF-) as the whole plot factor and time (days) as the split-plot factors using a mixed effect ANOVA model in the R nlme package (77). The least squares means were computed and separated with the Bonferroni method using the R emmeans package (78). 16S rRNA gene copies/mL were log10 transformed to meet normality and variance assumptions for ANOVA. To compare the no-biocide control at day zero and at the end of the experiment (day 56), the same model was used. To determine the differences between HF+ and HF- at day zero, an independent sample t-test was performed with data for only that time point. Microbial community alpha diversity (Chao 1, Simpson, Shannon, and Observed species) values were rank transformed and compared using the same model as for 16S rRNA gene copies/mL. Finally, microbial community beta diversity weighted UniFrac distance matrix was used to compare temporal differences between HF+ and HF- microcosms before and after DBNPA addition were applying a nested PERMANOVA with 999 permutations using the adonis command in the Vegan (74) R package. All statistical tests were performed using R, and p-value significance was set at p= 0.05. See supplemental methods for R-scripts used.

Quantification of DBNPA using HPLC-DAD

Every week, 1 mL of microcosm water was collected to compare the difference between the rates of abiotic and biotic DBNPA degradation in HF+ and HF- microcosms. After collection, samples were filter-sterilized using 0.2 µm nylon filter, acidified to pH 2.5 with phosphoric acid to minimize hydrolysis of DBNPA as described by Blanchard *et al.* (1987), and were then frozen at -20°C until analysis.

DBNPA quantification was performed with an Agilent 1200 HPLC system using a modified method described by Blanchard *et al.* (1987). An Agilent Eclipse XDB-C18 column (5 µm, 4.6 x 150 mm) was used for separation with a flowrate of 1mL/min and a diode array detector (DAD) was set at 210 nm for detection. The mobile phases and elution gradient were as follows: The initial composition was 75% deionized water (adjusted to pH 2.5 with phosphoric acid; eluent A) and 25% acetonitrile (eluent B), and eluent B increased linearly to 60% over 6 min and further to 85% over an additional 4 min time period. Eluent B was held at 85% for 1 min before the column was equilibrated to initial conditions.

Detection of DBNPA Degradation Products Using Nano-High Performance Liquid Chromatography-High-Resolution Mass Spectrometry

Filtered stream water samples were kept frozen in amber bottles in the dark at -20°C until analysis by nano-liquid chromatography-high-resolution mass spectrometry (nano-HPLC-HRMS). Measurements were collected using a Dionex UltiMate 3000 HPLC pump (ThermoFisher Scientific) coupled to an LTQ-Orbitrap Velos Pro mass spectrometer (ThermoFisher Scientific) equipped with a nano-electrospray ionization (ESI) source (Proxeon, Denmark) operated in positive mode under direct control of the XCalibur software, v2.2 SP1.48 (ThermoFisher Scientific). The nano-electrospray column/emitter was prepared manually in-house using 100 µm i.d. fused-silica (Polymicro Technologies) which was laser-pulled and pressure-packed to 20 cm with Kinetex C18-RP material (5 µm, 100 Å, Phenomenex). The column was aligned in front of the MS capillary inlet, and 300 nL of the sample was manually injected directly onto the column. LC/MS-grade acetonitrile (ACN) and water (both degassed) were purchased from EMD Millipore, and formic acid (FA) from Sigma-Aldrich. Nano-flow rates were achieved with a split-flow setup prior to the injection loop (~250 nL min^{-1} at the nano-spray tip) and separations were conducted by initially holding at 100% A (95% ACN/5% H_2O/0.1%

FA) for 5 min, increasing linearly over 60 min to 100% B (70% ACN/30% H_2O/0.1% FA), and then holding at 100% B for 5 min before re-equilibrating the column at 100% A for 20 min prior the next injection.

The mass spectrometer was externally calibrated for mass accuracy on the day of analysis using the positive calibration solution (Pierce, ThermoFisher Scientific). The ESI source capillary voltage was set to 3.0 kV and the capillary temperature to 275°C. High-resolution full scans were acquired in centroid mode at a resolving power of 30,000 over a mass range of 50 – 1000 *m/z*. Fragmentation data (MS^2) were also collected using collision-induced dissociation (CID, $He_{(g)}$) and a data-dependent acquisition approach on the top 5 most abundant ions in each MS^1 full scan. High-resolution (15,000 resolving power) MS^2 spectra were collected using a 2 *m/z* precursor isolation width, and an optimized 30% normalized CID energy for fragmentation. Raw LC/MS data were analyzed using the Thermo XCalibur Qual Software. Integrated LC peak areas were obtained from the extracted ion chromatograms (10 ppm tolerance).

Accession Numbers and Data Availability

Mass spectrometry data was uploaded to the Center for Computation Mass Spectrometry (UCSD) online database MassIVE. The MassIVE ID number is MSV000082488. Microbial 16S rRNA gene amplicon sequences for both DBNPA treated microcosm and the glutaraldehyde treated microcosms were deposited in NCBI Sequence Read Archive (SRA) in SRA accession SRP151211 under BioProject PRJNA476929 as Biosamples SAMN09459387 to SAMN09459570, and SAMN09475542 to SAMN09475579.

ACKNOWLEDGMENTS

This research was funded by the Methane Center in the Institute for a Secure and Sustainable Environment (http://isse.utk.edu/methane/), the Bredesen Center at the University of Tennessee, and the National Science Foundation CBET awards 1805152 (University of Tennessee), 1804685 (Michigan Technological University), and 1805549 (Juniata College).

SUPPORTING INFORMATION

Figure S1: DBNPA and known degradation products.

Figure S2: Microbial Community Shifts Over Time. A) Phylum, B) Genus

Figure S3: Biotic and abiotic degradation of DBNPA over time. Data is shown averaged by HF+ and HF-.

Figure S4: Biotic and abiotic DBNPA degradation over time. Data is shown by water source location.

Figure S5: High-resolution mass spectrum of DBNPA standard.

Figure S6: Number of brominated species detected by nano-HPLC-HRMS in two HF- (left) and two HF+ (right) sets of microcosm samples, biotic and abiotic, from days 0, 7, 14, 21, and 28.

Figure S7: Summed peak areas for all brominated compounds at each time point (0, 7, 14, and 28 days), normalized to each sample set (stream), analyzed by nano-HPLC-HRMS.

Table S1: DESeq2 results, OTU enrichment 7 days after glutaraldehyde addition

Table S2: DESeq2 results HF- vs HF+ enrichment at day 7

Table S3: DESeq2 results, enriched OTU at day 21 vs 0

Table S4: DESeq2 results, enriched OTU at day 35 vs 0

Table S5: DESeq2 results, enriched OTU at day 49 vs 0

Table S6: DESeq2 results, enriched OTU at day 56 vs 0

Table S7: DESeq2 results HF- vs HF+ enrichment at day 21

Table S8: DESeq2 results HF- vs HF+ enrichment at day 35

Table S9: DESeq2 results HF- vs HF+ enrichment at day 49

Table S10: DESeq2 results HF- vs HF+ enrichment at day 56

Table S11: DESeq2 results day 56 no-GA vs no-GA

Table S12: DESeq2 results day 56 vs day 56 no-DBNPA

Table S13: Putative DBNPA brominated degradation products detected by nano-HPLC-HRMS.

Table S14: Total Organic Carbon (TOC) concentration in source water prior to DBNPA addition.

Table S15: Geological coordinates and watershed physiochemical parameters.

REFERENCES

1. EIA US. 2017. Annual Energy Outlook 2017 with Projections to 2035, *on* U.S. Department of Energy, Energy Information Administration. https://www.eia.gov/outlooks/aeo/pdf/0383(2017).pdf. Accessed
2. Kahrilas GA, Blotevogel J, Stewart PS, Borch T. 2014. Biocides in hydraulic fracturing fluids: A critical review of their usage, mobility, degradation, and toxicity. Environ Sci Technol 49:16-32.
3. Struchtemeyer CG, Elshahed MS. 2012. Bacterial communities associated with hydraulic fracturing fluids in thermogenic natural gas wells in North Central Texas, USA. FEMS Microbiology Ecology 81:13-25.
4. Muyzer G, Stams AJM. 2008. The ecology and biotechnology of sulphate-reducing bacteria. Nature Reviews Microbiology 6:441-454.
5. Kahrilas GA, Blotevogel J, Corrin ER, Borch T. 2016. Downhole Transformation of the Hydraulic Fracturing Fluid Biocide Glutaraldehyde: Implications for Flowback and Produced Water Quality. Environ Sci Technol 50:11414-11423.
6. Stringfellow WT, Domen JK, Camarillo MK, Sandelin WL, Borglin S. 2014. Physical, chemical, and biological characteristics of compounds used in hydraulic fracturing. Journal of hazardous materials 275:37-54.
7. Williams TM, McGinley HR. 2010. Deactivation Of Industrial Water Treatment Biocides, abstr CORROSION 2010, San Antonio, Texas, 2010/1/1/. NACE International, NACE.
8. Paulus W. 2005. Directory of microbicides for the protection of materials: a handbook. Springer Science & Business Media.
9. Wolf PA, Sterner PW. 1972. 2,2-dibromo-3-nitrilopropionamide, a compound with slimicidal activity. Appl Microbiol 24:581-4.
10. EPA US. 1994. Reregistration Eligibility Decision (RED) 2,2,-dibromo-3-nitrilopropionamide (DBNPA). https://archive.epa.gov/pesticides/reregistration/web/pdf/3056.pdf.
11. Trexler R, Solomon C, Brislawn CJ, Wright JR, Rosenberger A, McClure EE, Grube AM, Peterson MP, Keddache M, Mason OU, Hazen TC, Grant CJ, Lamendella R. 2014. Assessing impacts of unconventional natural gas extraction on microbial communities in headwater stream ecosystems in Northwestern Pennsylvania. Frontiers in Microbiology 5:522.
12. Ulrich N, Kirchner V, Drucker R, Wright JR, McLimans CJ, Hazen TC, Campa MF, Grant CJ, Lamendella R. 2018. Response of Aquatic Bacterial Communities to Hydraulic Fracturing in Northwestern Pennsylvania: A Five-Year Study. Scientific Reports 8:5683.
13. Blanchard FA, Gonsior SJ, Hopkins DL. 1987. 2,2-Dibromo-3-nitrilopropionamide (DBNPA) chemical degradation in natural waters:

Experimental evaluation and modeling of competitive pathways. Water Research 21:801-807.

14. Richardson SD. 2003. Disinfection by-products and other emerging contaminants in drinking water. TrAC Trends in Analytical Chemistry 22:666-684.

15. Exner JH, Burk GA, Kyriacou D. 1973. Rates and Products of Decomposition of 2,2-Dibromo-3-Nitrilopropionamide. Journal of Agricultural and Food Chemistry 21:838-842.

16. Grant CJ, Weimer AB, Marks NK, Perow ES, Oster JM, Brubaker KM, Trexler RV, Solomon CM, Lamendella R. 2015. Marcellus and mercury: Assessing potential impacts of unconventional natural gas extraction on aquatic ecosystems in northwestern Pennsylvania. J Environ Sci Health A Tox Hazard Subst Environ Eng 50:482-500.

17. EPA US. 2012. Study of the potential impacts of hydraulic fracturing on drinking water resources. Agency USEP, https://www.epa.gov/sites/production/files/documents/hf-report20121214.pdf.

18. Gross SA, Avens HJ, Banducci AM, Sahmel J, Panko JM, Tvermoes BE. 2013. Analysis of BTEX groundwater concentrations from surface spills associated with hydraulic fracturing operations. Journal of the Air & Waste Management Association 63:424-432.

19. Drollette BD, Hoelzer K, Warner NR, Darrah TH, Karatum O, O'Connor MP, Nelson RK, Fernandez LA, Reddy CM, Vengosh A, Jackson RB, Elsner M, Plata DL. 2015. Elevated levels of diesel range organic compounds in groundwater near Marcellus gas operations are derived from surface activities. Proceedings of the National Academy of Sciences 112:13184-13189.

20. Hildenbrand ZL, Carlton DD, Fontenot BE, Meik JM, Walton JL, Taylor JT, Thacker JB, Korlie S, Shelor CP, Henderson D, Kadjo AF, Roelke CE, Hudak PF, Burton T, Rifai HS, Schug KA. 2015. A Comprehensive Analysis of Groundwater Quality in The Barnett Shale Region. Environ Sci Technol 49:8254-8262.

21. Akob DM, Mumford AC, Orem W, Engle MA, Klinges JG, Kent DB, Cozzarelli IM. 2016. Wastewater Disposal from Unconventional Oil and Gas Development Degrades Stream Quality at a West Virginia Injection Facility. Environ Sci Technol 50:5517-5525.

22. Orem W, Varonka M, Crosby L, Haase K, Loftin K, Hladik M, Akob DM, Tatu C, Mumford A, Jaeschke J, Bates A, Schell T, Cozzarelli I. 2017. Organic geochemistry and toxicology of a stream impacted by unconventional oil and gas wastewater disposal operations. Applied Geochemistry 80:155-167.

23. Shade A, Peter H, Allison SD, Baho DL, Berga M, Burgmann H, Huber DH, Langenheder S, Lennon JT, Martiny JB, Matulich KL, Schmidt TM, Handelsman J. 2012. Fundamentals of microbial community resistance and resilience. Front Microbiol 3:417.

24. Dow. n.d. Delivering Value with an Optimized Microbial Control Program in Oil and Gas Operations. http://msdssearch.dow.com/PublishedLiteratureDOWCOM/dh_097e/0901b

8038097eef2.pdf?filepath=microbial/pdfs/noreg/253-02697.pdf&fromPage=GetDoc. Accessed April 30.

25. Findlay S. 2010. Stream microbial ecology. Journal of the North American Benthological Society 29:170-181.

26. Zeglin LH. 2015. Stream microbial diversity in response to environmental changes: review and synthesis of existing research. Front Microbiol 6:454.

27. Smith MB, Rocha AM, Smillie CS, Olesen SW, Paradis C, Wu LY, Campbell JH, Fortney JL, Mehlhorn TL, Lowe KA, Earles JE, Phillips J, Techtmann SM, Joyner DC, Elias DA, Bailey KL, Hurt RA, Preheim SP, Sanders MC, Yang J, Mueller MA, Brooks S, Watson DB, Zhang P, He ZL, Dubinsky EA, Adams PD, Arkin AP, Fields MW, Zhou JZ, Alm EJ, Hazen TC. 2015. Natural Bacterial Communities Serve as Quantitative Geochemical Biosensors. Mbio 6.

28. Campa MF, Techtmann SM, Gibson CM, Zhu X, Patterson M, Garcia de Matos Amaral A, Ulrich N, Campagna SR, Grant CJ, Lamendella R, Hazen TC. 2018. Impacts of Glutaraldehyde on Microbial Community Structure and Degradation Potential in Streams Impacted by Hydraulic Fracturing. Environ Sci Technol 52:5989-5999.

29. Moeseneder MM, Arrieta JM, Herndl GJ. 2005. A comparison of DNA- and RNA-based clone libraries from the same marine bacterioplankton community. FEMS Microbiol Ecol 51:341-52.

30. Hazen TC. 2018. Cometabolic Bioremediation. Consequences of Microbial Interactions with Hydrocarbons, Oils, and Lipids. *In* Steffan R (ed), Biodegradation and Bioremediation doi:https://doi.org/10.1007/978-3-319-44535-9_5-1. Springer International Publishing AG.

31. Swan BK, Martinez-Garcia M, Preston CM, Sczyrba A, Woyke T, Lamy D, Reinthaler T, Poulton NJ, Masland EDP, Gomez ML, Sieracki ME, DeLong EF, Herndl GJ, Stepanauskas R. 2011. Potential for Chemolithoautotrophy Among Ubiquitous Bacteria Lineages in the Dark Ocean. Science 333:1296-1300.

32. Sanford RA, Chowdhary J, Loffler FE. Organohalife-Respiring *Deltaproteobacteria*. *In* Adrian L, Loeffler FE (ed), Organohalide-Respiring Bacteria doi:10.1007/978-3-662-49875-0. Springer.

33. Kostka JE, Prakash O, Overholt WA, Green SJ, Freyer G, Canion A, Delgardio J, Norton N, Hazen TC, Huettel M. 2011. Hydrocarbon-Degrading Bacteria and the Bacterial Community Response in Gulf of Mexico Beach Sands Impacted by the Deepwater Horizon Oil Spill. Applied and Environmental Microbiology 77:7962-7974.

34. Levy SB. 2002. Active efflux, a common mechanism for biocide and antibiotic resistance. J Appl Microbiol 92 Suppl:65S-71S.

35. Poole K. 2007. Efflux pumps as antimicrobial resistance mechanisms. Annals of Medicine 39:162-176.

36. Vikram A, Bomberger JM, Bibby KJ. 2015. Efflux as a Glutaraldehyde Resistance Mechanism in Pseudomonas fluorescens and Pseudomonas aeruginosa Biofilms. Antimicrobial Agents and Chemotherapy 59:3433-3440.

37. Vikram A, Lipus D, Bibby K. 2014. Produced water exposure alters bacterial response to biocides. Environ Sci Technol 48:13001-13009.

38. Comte J, Lindström ES, Eiler A, Langenheder S. 2014. Can marine bacteria be recruited from freshwater sources and the air? The ISME Journal 8:2423-2430.

39. Mumford AC, Akob DM, Klinges JG, Cozzarelli IM. 2018. Common hydraulic fracturing fluid additives alter the structure and function of anaerobic microbial communities. Applied and Environmental Microbiology.

40. Chen See JR, Ulrich N, Nwanosike H, McLimans CJ, Tokarev V, Wright JR, Campa MF, Grant CJ, Hazen TC, Niles JM, Ressler D, Lamendella R. 2018. Bacterial Biomarkers of Marcellus Shale Activity in Pennsylvania. Frontiers in Microbiology 9.

41. Mouser PJ, Borton M, Darrah TH, Hartsock A, Wrighton KC. 2016. Hydraulic fracturing offers view of microbial life in the deep terrestrial subsurface. FEMS Microbiology Ecology doi:10.1093/femsec/fiw166.

42. Zhang XX, Zhang T, Fang HH. 2009. Antibiotic resistance genes in water environment. Appl Microbiol Biotechnol 82:397-414.

43. Russell AD. 2001. Mechanisms of bacterial insusceptibility to biocides. Am J Infect Control 29:259-61.

44. Setlow P. 2006. Spores of Bacillus subtilis: their resistance to and killing by radiation, heat and chemicals. J Appl Microbiol 101:514-25.

45. Furuhata K, Kato Y, Goto K, Hara M, Yoshida S-i, Fukuyama M. 2006. Isolation and Identification of Methylobacterium Species from the Tap Water in Hospitals in Japan and Their Antibiotic Susceptibility. Microbiology and Immunology 50:11-17.

46. Gan HM, Hudson AO, Rahman AYA, Chan KG, Savka MA. 2013. Comparative genomic analysis of six bacteria belonging to the genus Novosphingobium: insights into marine adaptation, cell-cell signaling and bioremediation. BMC genomics 14:431-431.

47. Vikram A, Lipus D, Bibby K. 2016. Metatranscriptome analysis of active microbial communities in produced water samples from the Marcellus Shale. Microb Ecol 72:571-81.

48. Rogers JD, Ferrer I, Tummings SS, Bielefeldt AR, Ryan JN. 2017. Inhibition of Biodegradation of Hydraulic Fracturing Compounds by Glutaraldehyde: Groundwater Column and Microcosm Experiments. Environ Sci Technol 51:10251-10261.

49. McLaughlin MC, Borch T, Blotevogel J. 2016. Spills of Hydraulic Fracturing Chemicals on Agricultural Topsoil: Biodegradation, Sorption, and Co-contaminant Interactions. Environ Sci Technol 50:6071-8.

50. Matzek LW, Carter KE. 2017. Sustained persulfate activation using solid iron: Kinetics and application to ciprofloxacin degradation. Chemical Engineering Journal 307:650-660.

51. McDonnell G, Russell AD. 1999. Antiseptics and disinfectants: activity, action, and resistance. Clin Microbiol Rev 12:147-79.

52. Villanueva CM, Cordier S, Font-Ribera L, Salas LA, Levallois P. 2015. Overview of Disinfection By-products and Associated Health Effects. Current Environmental Health Reports 2:107-115.

53. Li X-F, Mitch WA. 2018. Drinking Water Disinfection Byproducts (DBPs) and Human Health Effects: Multidisciplinary Challenges and Opportunities. Environ Sci Technol 52:1681-1689.

54. Hladik ML, Focazio MJ, Engle M. 2014. Discharges of produced waters from oil and gas extraction via wastewater treatment plants are sources of disinfection by-products to receiving streams. Science of The Total Environment 466-467:1085-1093.

55. Akyon B, McLaughlin M, Hernández F, Blotevogel J, Bibby K. 2019. Characterization and biological removal of organic compounds from hydraulic fracturing produced water. Environmental Science: Processes & Impacts.

56. Grant CJ, Lutz AK, Kulig AD, Stanton MR. 2016. Fracked ecology: Response of aquatic trophic structure and mercury biomagnification dynamics in the Marcellus Shale Formation. Ecotoxicology 25:1739-1750.

57. Janssen DB, Oppentocht JE, Poelarends GJ. 2001. Microbial dehalogenation. Curr Opin Biotechnol 12:254-8.

58. Mohn WW, Tiedje JM. 1992. Microbial reductive dehalogenation. Microbiol Rev 56:482-507.

59. Fetzner S, Lingens F. 1994. Bacterial dehalogenases: biochemistry, genetics, and biotechnological applications. Microbiol Rev 58:641-85.

60. Levis E. 2016. Texas Company Pays $93,710 settlement for polluting Clearfield County Creek. Pennsylvania Fish and Boat Commision., p *In* Pennsylvania Fish and Boat Commision. Harrisburg, PA. https://hero.epa.gov/hero/index.cfm/reference/details/reference_id/2447894.

61. PADEP. 2013. Oil and Gas Annual Report. Pennsylvania Department of Environmental Protection Office of Oil and Gas Management,

62. Dunlap K. 2011. Shale gas production and water resources in the eastern United States, *on* U.S. Senate Committee on Energy and Natural Resources Subcommittee on Water and Power. https://www.energy.senate.gov/public/index.cfm/files/serve?File_id=1CBE5C49-AA41-4BEC-A6B7-992068C59666. Accessed April 1, 2018.

63. Lutz AK, Grant CJ. 2016. Impacts of hydraulic fracturing development on macroinvertebrate biodiversity and gill morphology of net-spinning caddisfly (Hydropsychidae, Diplectrona) in northwestern Pennsylvania, USA. Journal of Freshwater Ecology 31:211-217.

64. Caporaso JG, Kuczynski J, Stombaugh J, Bittinger K, Bushman FD, Costello EK, Fierer N, Pena AG, Goodrich JK, Gordon JI, Huttley GA, Kelley ST, Knights D, Koenig JE, Ley RE, Lozupone CA, McDonald D, Muegge BD, Pirrung M, Reeder J, Sevinsky JR, Turnbaugh PJ, Walters WA, Widmann J, Yatsunenko T, Zaneveld J, Knight R. 2010. QIIME allows analysis of high-throughput community sequencing data. Nat Methods 7:335-6.

65. Edgar RC. 2010. Search and clustering orders of magnitude faster than BLAST. Bioinformatics 26:2460-1.

66. Edgar RC, Haas BJ, Clemente JC, Quince C, Knight R. 2011. UCHIME improves sensitivity and speed of chimera detection. Bioinformatics 27:2194-200.

67. DeSantis TZ, Hugenholtz P, Larsen N, Rojas M, Brodie EL, Keller K, Huber T, Dalevi D, Hu P, Andersen GL. 2006. Greengenes, a chimera-checked 16S rRNA gene database and workbench compatible with ARB. Appl Environ Microbiol 72:5069-72.
68. Caporaso JG, Bittinger K, Bushman FD, DeSantis TZ, Andersen GL, Knight R. 2010. PyNAST: a flexible tool for aligning sequences to a template alignment. Bioinformatics 26:266-7.
69. Wang Q, Garrity GM, Tiedje JM, Cole JR. 2007. Naive Bayesian classifier for rapid assignment of rRNA sequences into the new bacterial taxonomy. Appl Environ Microbiol 73:5261-7.
70. Paulson JN, Stine OC, Bravo HC, Pop M. 2013. Differential abundance analysis for microbial marker-gene surveys. Nature Methods 10:1200.
71. Lozupone C, Lladser ME, Knights D, Stombaugh J, Knight R. 2011. UniFrac: an effective distance metric for microbial community comparison. The ISME journal 5:169-172.
72. Vázquez-Baeza Y, Pirrung M, Gonzalez A, Knight R. 2013. EMPeror: a tool for visualizing high-throughput microbial community data. GigaScience 2:16-16.
73. McMurdie PJ, Holmes S. 2013. phyloseq: an R package for reproducible interactive analysis and graphics of microbiome census data. PLoS One 8:e61217.
74. Dixon P. 2003. VEGAN, a package of R functions for community ecology. Journal of Vegetation Science 14:927-930.
75. McMurdie PJ, Holmes S. 2014. Waste not, want not: why rarefying microbiome data is inadmissible. PLoS computational biology 10:e1003531-e1003531.
76. Love MI, Huber W, Anders S. 2014. Moderated estimation of fold change and dispersion for RNA-seq data with DESeq2. Genome Biol 15:550.
77. Pinheiro JB, D.; DebRoy, S.; Sarkar, D.; and R Core Team 2018. nlme: Linear and Nonlinear Mixed Effects Models. R package version 31-1311.
78. Lenth RL, J.; Herve, M. 2018. Estimated Marginal Means, aka Least-Square Means. R package version 112.

FIGURES AND LEGENDS

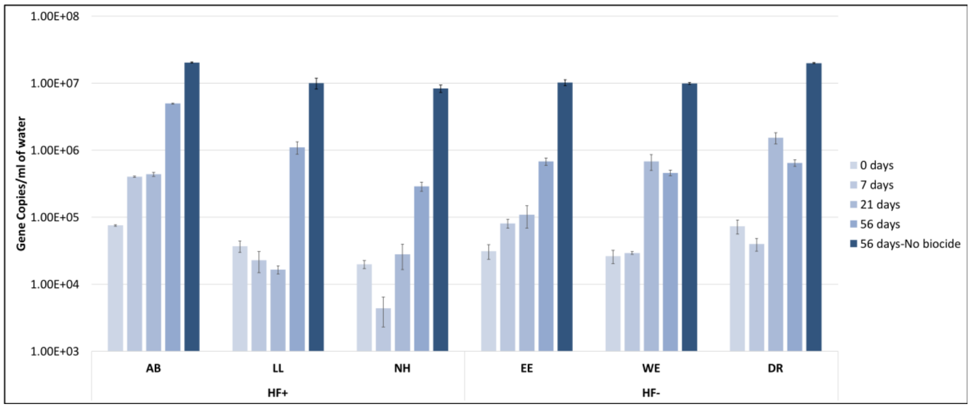

Figure 1. Impacts of DBNPA in abundance of 16S rRNA gene copies/mL over time. Data shown is divided by HF-impacted (first three clusters, Alex Branch (AB), Little Laurel (LL), Naval Hollow (NH)) and HF-unimpacted (East Elk (EE), West Elk (WE), Dixon Run (DR)) microcosms at day zero before DBNPA addition, day 7, 21, and 56 after DBNPA addition, and day 56 no-DBNPA added control. The bars are color on a gradient over time, with the last bar representing the no-DBNPA control at day 56. Each bar represents n=3, and the error bars represent one standard error.

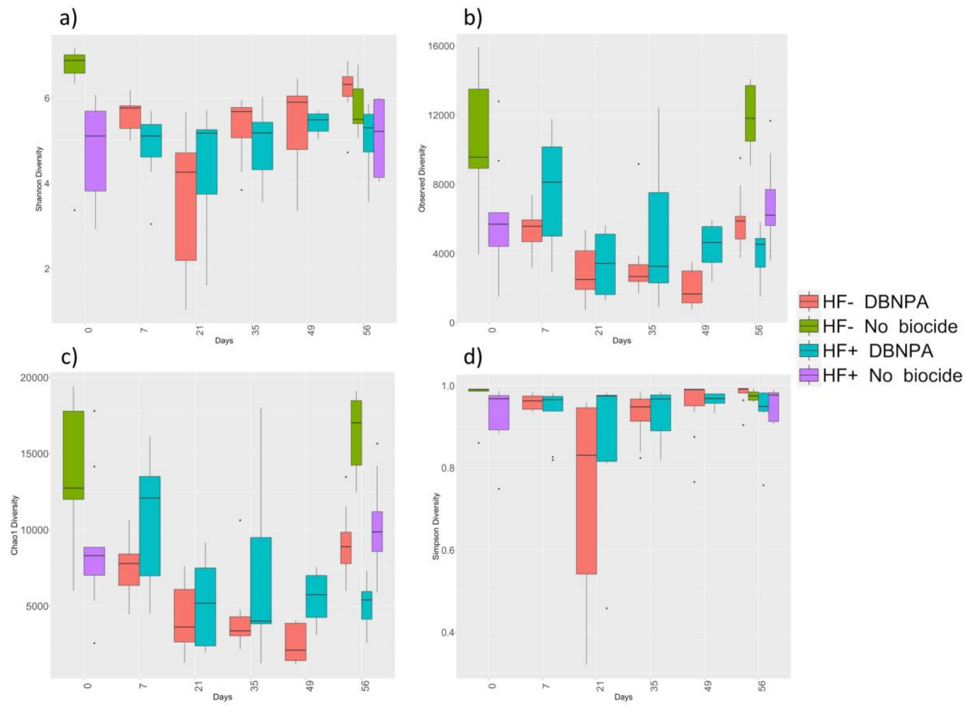

Figure 2. Four different richness and evenness alpha diversity estimators comparing HF-impacted and HF-unimpacted microcosms over time. The estimators used were (a) Shannon Diversity, (b) Observed Diversity, (c) Chao1, and (d) Simpson Diversity. Red and green represent HF-unimpacted microcosms. Red boxes represent the changes after DBNPA addition in HF-unimpacted (days 7 to 56), while the green boxes represent the alpha diversity without DBNPA addition in HF- (day zero and 56). Blue and purple boxes represent HF-impacted microcosms. Blue boxes represent the changes after DBNPA addition in HF-impacted (days 7 to 56), while the purple boxes represent the alpha diversity without DBNPA addition in HF- (day zero and 56). The box and whisker plot described the distribution of the data points. The beginning of the whiskers to the beginning of the box are the upper and lower quartiles. The box represents the interquartile range, which represents 50% of the data points (n=9). The vertical line inside the box represents the median.

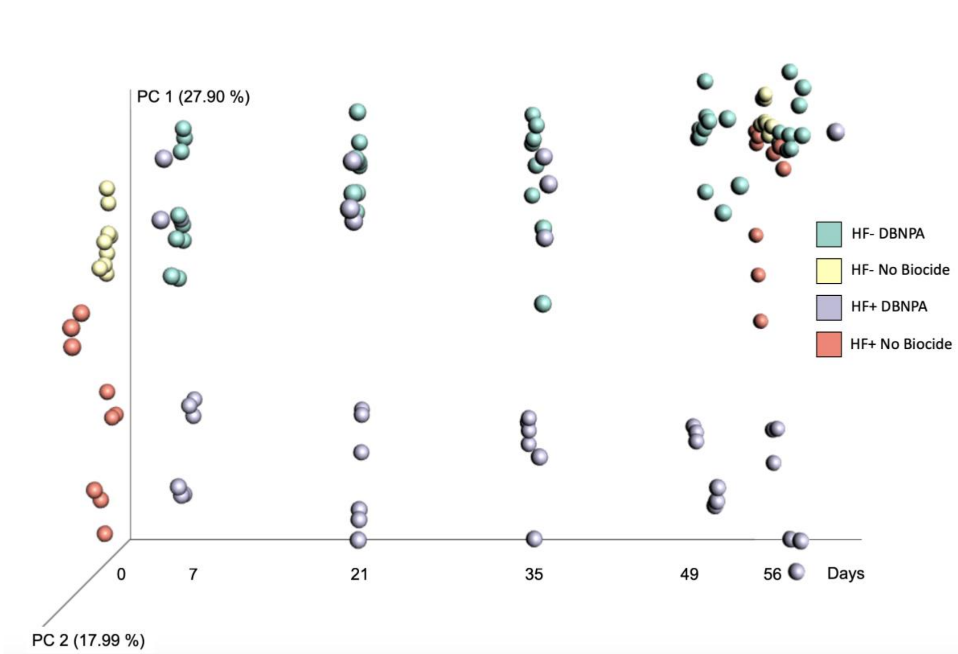

Figure 3. Directional Principal Coordinate Analysis (PCoA) plots of weighted UniFrac distances between microcosms. Samples were plotted on the x-axis from left to right according to days sampled, 0, 7, 21, 35, 49, and 56. Samples are colored by hydraulic fracturing (HF)-impact history and DBNPA addition. The green legend = HF-unimpacted plus DBNPA addition, yellow legend= HF-unimpacted without biocide addition, purple legend= HF-impacted plus DBNPA addition, and pink legend= HF-impacted without biocide addition. Samples without biocide addition were only measured day 0 and day 56.

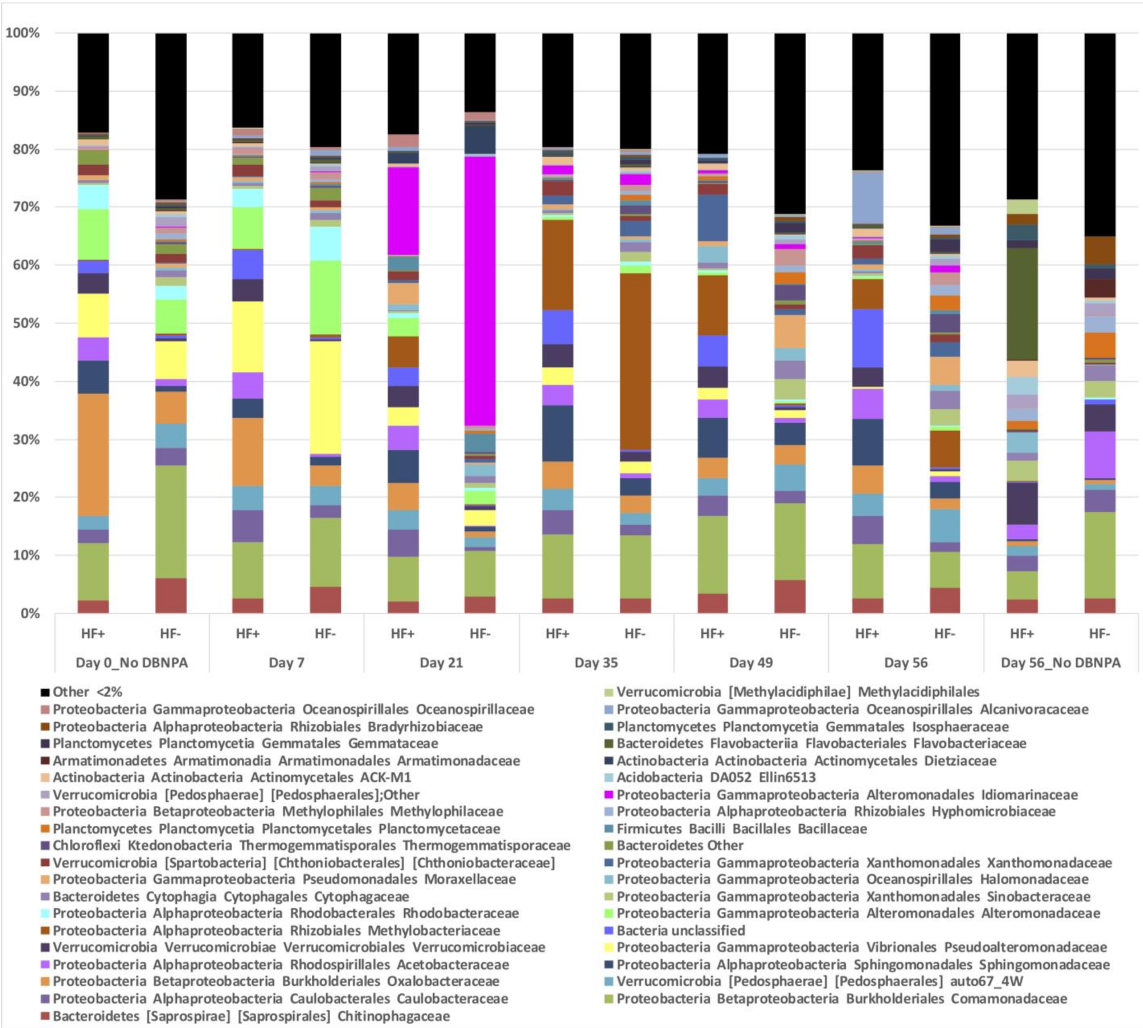

Figure 4. Temporal changes of microbial community relative abundance in averaged hydraulic fracturing-impacted (HF+) and hydraulic fracturing-unimpacted (HF-) microcosms treated with the biocide DBNPA. Microbial taxa are summarized to the Family level.

A)

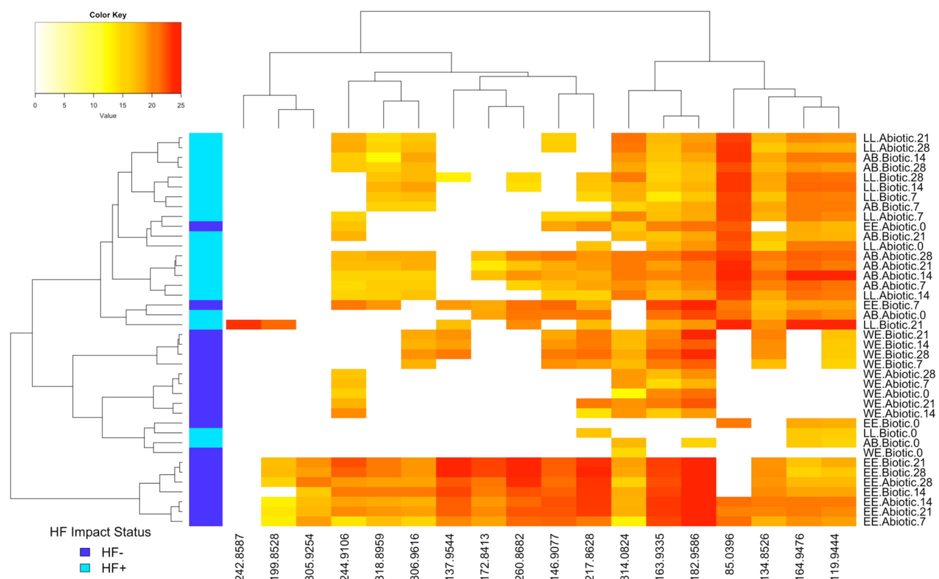
Color Key
0
5
10
15
20
25
Value
HF Impact Status
HF-
HF+
LL.Abiotic.21
LL.Abiotic.28
AB.Biotic.14
AB.Biotic.28
LL.Biotic.28
LL.Biotic.14
LL.Biotic.7
AB.Biotic.7
LL.Abiotic.7
EE.Abiotic.0
AB.Biotic.21
LL.Abiotic.0
AB.Abiotic.28
AB.Abiotic.21
AB.Abiotic.14
AB.Abiotic.7
LL.Abiotic.14
EE.Biotic.7
AB.Abiotic.0
LL.Biotic.21
WE.Biotic.21
WE.Biotic.14
WE.Biotic.28
WE.Biotic.7
WE.Abiotic.28
WE.Abiotic.7
WE.Abiotic.0
WE.Abiotic.21
WE.Abiotic.14
EE.Biotic.0
LL.Biotic.0
AB.Biotic.0
WE.Biotic.0
EE.Biotic.21
EE.Biotic.28
EE.Abiotic.28
EE.Biotic.14
EE.Abiotic.14
EE.Abiotic.21
EE.Abiotic.7
242.8587
199.8528
305.9254
244.9106
318.8959
306.9616
137.9544
172.8413
260.8682
146.9077
217.8628
314.0824
163.9335
182.9586
85.0396
134.8526
164.9476
119.9444

B)

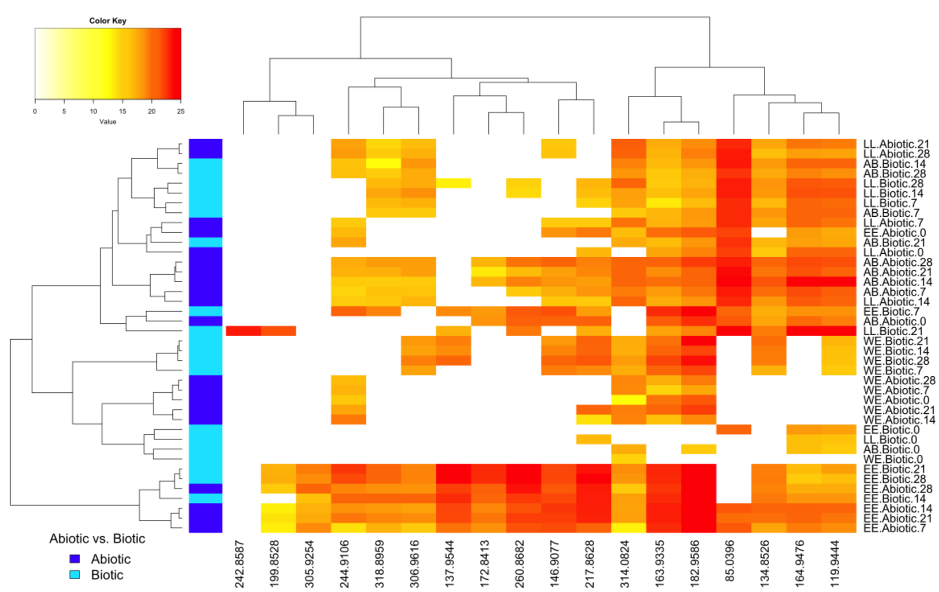
Color Key
0
5
10
15
20
25
Value
Abiotic vs. Biotic
Abiotic
Biotic
LL.Abiotic.21
LL.Abiotic.28
AB.Biotic.14
AB.Biotic.28
LL.Biotic.28
LL.Biotic.14
LL.Biotic.7
AB.Biotic.7
LL.Abiotic.7
EE.Abiotic.0
AB.Biotic.21
LL.Abiotic.0
AB.Abiotic.28
AB.Abiotic.21
AB.Abiotic.14
AB.Abiotic.7
LL.Abiotic.14
EE.Biotic.7
AB.Abiotic.0
LL.Biotic.21
WE.Biotic.21
WE.Biotic.14
WE.Biotic.28
WE.Biotic.7
WE.Abiotic.28
WE.Abiotic.7
WE.Abiotic.0
WE.Abiotic.21
WE.Abiotic.14
EE.Biotic.0
LL.Biotic.0
AB.Biotic.0
WE.Biotic.0
EE.Biotic.21
EE.Biotic.28
EE.Abiotic.28
EE.Biotic.14
EE.Abiotic.14
EE.Abiotic.21
EE.Abiotic.7
242.8587
199.8528
305.9254
244.9106
318.8959
306.9616
137.9544
172.8413
260.8682
146.9077
217.8628
314.0824
163.9335
182.9586
85.0396
134.8526
164.9476
119.9444

Figure 5. Heat maps of the normalized $\log_2$ peak areas for brominated species detected by nano-HPLC-HRMS. The dendrograms cluster samples using the Ward method of agglomeration. Rows represent samples (described by stream location, condition, and day of collection) and columns represent m/z ratios of the brominates species detected. The top dendrogram is clustered by brominated species that varied similarly across the data set. A) The left dendrogram clusters first by HF+ (light blue) or HF- (dark blue) streams, and then by abiotic and biotic microcosms. B) The left dendrogram clusters by abiotic (dark blue) and biotic (light blue) samples.

Table 1. Nested PERMANOVA of weighted UniFrac distances

Source of Variation	Degrees of Freedom	Sum of Squares	Mean Square	F. Model	R2	P value
HF_ImpactStatus	1	0.9515	0.95148	30.3412	0.15771	0.001
Biocide	1	0.4506	0.45056	14.3678	0.07468	0.001
Biocide:Days	2	0.7840	0.39199	12.5000	0.12995	0.001
HF_ImpactStatus: Biocide	1	0.1381	0.13806	4.4024	0.02288	0.001
HF_ImpactStatus: Biocide: Days	2	0.1653	0.08266	2.6359	0.02740	0.001
Residuals	113	3.5436	0.03136		0.58737	
Total	120	6.0330			1.00000	